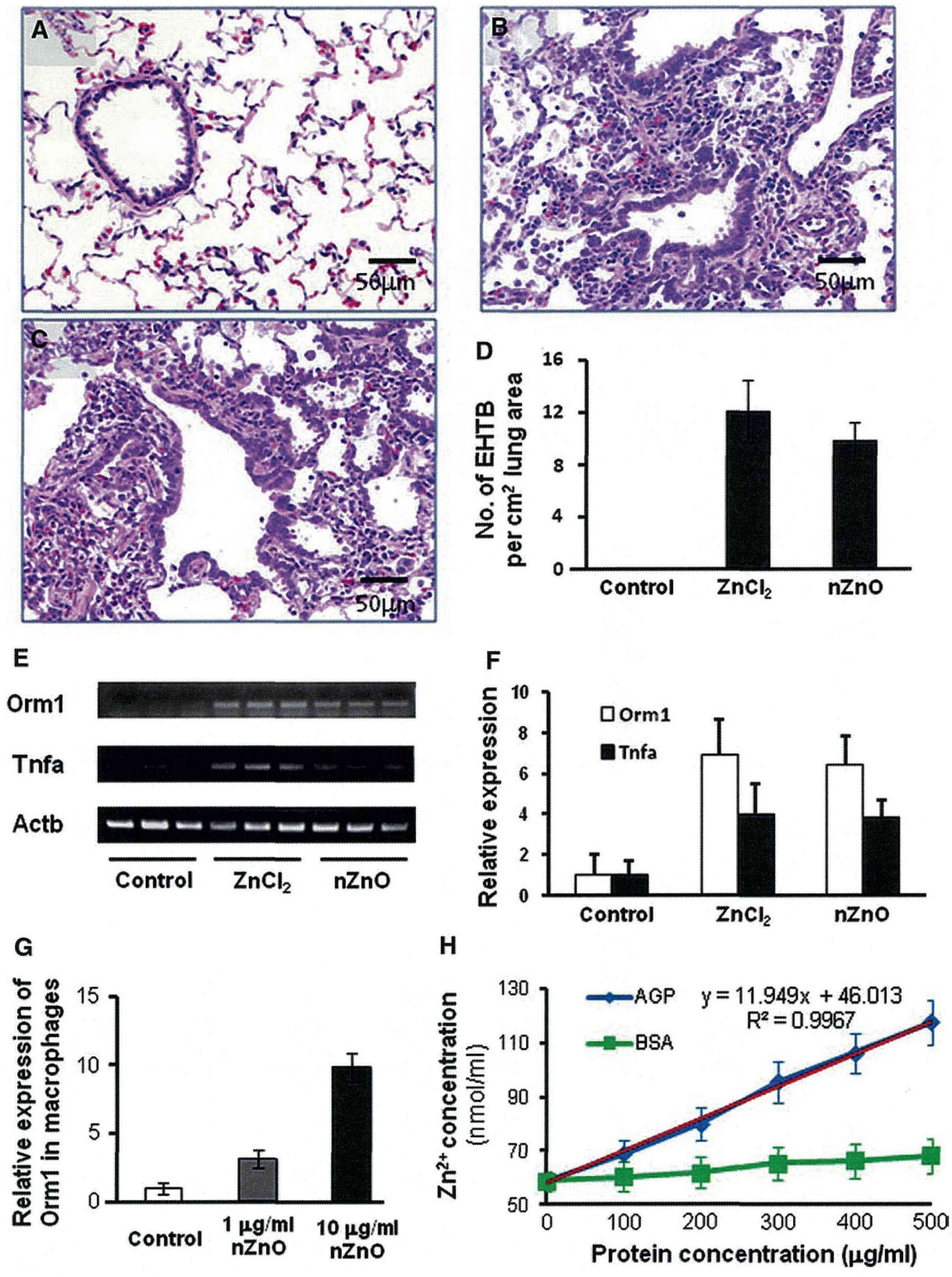

Fig. 4 Similar effects of $ZnCl_2$ solution and nZnO in induction of EHTB and FAIP in wild-type rats. **a** H&E-stained slides of the lungs of rats treated with vehicle; **b** with nZnO; and **c** with $ZnCl_2$ solution, showing EHTB and FAIP; **d** comparable number of EHTB per square centimeter of the lung tissues induced by treatment of $ZnCl_2$ and nZnO; **e** gene expression determined by RT-PCR of Orm1 and Tnfa, with Actb gene as an internal control; **f** real-time PCR analysis of gene expression of Orm1 and Tnfa, which was normalized with Actb expression; **g** induction of Orm1 expression in primary alveolar macrophages exposed to nZnO; and **h** effect of human alpha 1 acid glycoprotein (AGP) and bovine serum albumin (BSA) on dissolution of nZnO in vitro

examination of serum markers for tissue and organ injuries indicated no significant changes compared to the vehicle group (Table S3). Administration of nZnO or $ZnCl_2$ to the lung led to a transient increase in serum Zn^{2+} concentration which returned to normal levels within 2 weeks after administration. The elevated serum Zn^{2+} did not affect the homeostasis of the other ions examined (Table S4).

Discussion

In vivo nanomaterial toxicity usually implicates oxidative stress, inflammation (Nel et al. 2006), and other biological responses depending on the individual nanomaterial. In vitro assays related to carcinogenicity, such as mammalian cell transformation and gene mutation assays, cannot represent the complex in vivo processes of different biological alterations and are not always suitable for risk assessment of nanomaterial carcinogenicity. In the present study, we tested the carcinogenic activity of nZnO in H*ras*128 rats by an initiation–promotion protocol, by which we previously found promotion effect of nanosized titanium dioxide on DHPN-induced lung and mammary carcinogenesis (Xu et al. 2010). nZnO did not show any promotion effects on lung proliferative or neoplastic lesions, indicating that nZnO is not carcinogenetic. Also, nZnO did not promote DHPN-induced mammary carcinogenesis.

On the other hand, nZnO was found to induce EHTB in H*ras*128 rats and wild-type SD rats. EHTB is a proliferative lesion of the terminal bronchiolar epithelium. It should be noted that the localization of EHTB was independent from that of DHPN-induced alveolar cell hyperplasia. This observation clearly indicates that the DHPN-induced alveolar cell hyperplasia and EHTB have different etiology, the latter being induced by nZnO. We also observed 2 cases of alveolar cell hyperplasia out of 6 cases in the nZnO alone group. This is not significant and thus considered to be spontaneous or an inflammation-associated event. The EHTB lesions regressed when administration of nZnO was discontinued and completely disappeared after 12 weeks. Along with EHTB, the interstitial inflammatory changes often observed surrounding the EHTB lesions also regressed. Our data and other reports (Cho et al. 2011) indicate that the EHTB lesions do not progress directly to cancers but are reactive proliferation associated with inflammatory events. Similar reversible inflammatory changes in the bronchoalveolar lavage fluids by administration of nanoscale or fine ZnO particles via inhalation or intratracheal instillation have previously been reported (Warheit et al. 2009).

nZnO particles were not found in alveolar macrophages, in the lung tissue, or in other organs, suggesting that the particles were dissolved to Zn^{2+}. Accordingly, we conducted experiments to determine whether Zn^{2+} would induce similar lesions. $ZnCl_2$ solution induced closely similar lung lesions and gene expression profiles as nZnO, demonstrating that the observed lung lesions were caused by Zn^{2+}. This was confirmed by increased Zn^{2+} level in the lung and serum after administration of nZnO. Interestingly, treatment with nZnO up-regulated the expression of the Omr1 gene in both the lung and the alveolar macrophages, and in vitro addition of Omr1-encoded AGP dose-dependently promoted nZnO dissolution. After Zn^{2+} was cleared from the lung, the EHTB and FAIP lesions disappeared, and this was evidenced by the positive correlation of EHTB number with Zn^{2+} content in the lung. Dissolution of nZnO has been reported to be particle size- and pH-dependent (Mudunkotuwa et al. 2012). Increased Omr1 expression possibly alters the microenvironment of the alveolar macrophages and the lung which accelerates nZnO dissolution. The elevated Zn^{2+} from nZnO dissolution possibly interferes with zinc ion homeostasis and leads to cytotoxic effects (Kao et al. 2012).

According to OSHA, the permissible exposure limit for zinc oxide particles is 15 mg/m^3 of air for total dust and 5 mg/m^3 for the respirable fraction (http://www.osha.gov/SLTC/healthguidelines/zincoxide/recognition.html). The inhalation exposure limit per kilogram of body weight per day for the respirable fraction is 192 μg, calculated from 6,000 ml of minute respiratory volume and 8 working hours for a 75 kg body weight worker. The dosing in the carcinogenesis study of the present study was approximately 35.5 and 71 μg/kg body weight a day (calculated from 125 to 250 μg every two weeks for a 250 g rat) and is lower than the OSHA limit for humans. Since nZnO has more potential to be ionized than larger ZnO particles because of its higher surface area (Mudunkotuwa et al. 2012), this feature should be taken into regulatory consideration.

It has been estimated that engineered nanomaterials will become a $1 trillion enterprise by 2015 (Nel et al. 2006), and ensuring health and environmental safety is a challenging task to the nanotechnology industry. Among numerous engineered nanomaterials, metal based or carbon based, most of which have been shown to have toxic effects to at least some extent, nZnO is a promising nanomaterial for biomedical applications. The results of the present study indicate that, although nZnO induced reversible lung toxicity, it did not cause carcinogenic or chronic progressive inflammatory lesions. Also, since it is biodegradable to ions, nZnO is easily cleared from the body (Rasmussen et al. 2010). Our study also suggests that the toxic effects of nZnO can be further decreased if efforts such as proper dosing and surface coating are made to lower the Zn^{2+} release from nZnO.

In conclusion, treatment of nZnO by IPS did not promote lung and mammary carcinogenesis in our carcinogenesis model. Although nZnO induced EHTB and FAIP, the lesions regressed rapidly along with clearance of surplus Zn^{2+} from the lung and serum. Thus, from a toxicological viewpoint, under the present experimental conditions, exposure of the lung to nZnO does not cause progressive neoplastic development or chronic fibrosis in the lung. These findings will be helpful in evaluating of the safety of nZnO used in biomedical applications, in which its use is of rather short duration, although long-term studies including inhalation studies are required to assess their occupational and environmental health hazards.

Acknowledgments This work was supported by Health and Labor Sciences Research Grants (Research on Risk of Chemical Substance 21340601, H21-kagaku-ippan-008, H24-kagaku-ippan-009 and H22-kagaku-ippan-005) from the Ministry of Health, Labor and Welfare, Japan. We thank A. Iezaki for her excellent secretarial assistance for the work.

Conflict of interest The authors declare that they have no conflict of interest.

References

Antonini JM, Lewis AB, Roberts JR, Whaley DA (2003) Pulmonary effects of welding fumes: review of worker and experimental animal studies. Am J Ind Med 43:350–360

Baldwin S, Odio MR, Haines SL, O'Connor RJ, Englehart JS, Lane AT (2001) Skin benefits from continuous topical administration of a zinc oxide/petrolatum formulation by a novel disposable diaper. J Eur Acad Dermatol Venereol 15(Suppl 1):5–11

Cho WS, Duffin R, Howie SE, Scotton CJ, Wallace WA, Macnee W, Bradley M, Megson IL, Donaldson K (2011) Progressive severe lung injury by zinc oxide nanoparticles; the role of Zn2+ dissolution inside lysosomes. Part Fibre Toxicol 8:27–43

Deng X, Luan Q, Chen W, Wang Y, Wu M, Zhang H, Jiao Z (2009) Nanosized zinc oxide particles induce neural stem cell apoptosis. Nanotechnology 20:115101

Drinker CK, Fairhall LT (1933) Zinc in relation to general and industrial hygiene. Public Health Rep 48:955–961

Fine JM, Gordon T, Chen LC, Kinney P, Falcone G, Beckett WS (1997) Metal fume fever: characterization of clinical and plasma IL-6 responses in controlled human exposures to zinc oxide fume at and below the threshold limit value. J Occup Environ Med 39:722–726

Fournier T, Medjoubi NN, Porquet D (2000) Alpha-1-acid glycoprotein. Biochim Biophys Acta 1482:157–171

Heinrich U, Fuhst R, Rittinghausen S, Creutzenberg O, Bellmann B, Koch K, Levsen K (1995) Chronic inhalation exposure of wistar rats and two different strains of mice to diesel engine exhaust, carbon black, and titanium dioxide. Inhalation Toxicol 7:533–556

Hughes G, McLean NR (1988) Zinc oxide tape: a useful dressing for the recalcitrant finger-tip and soft-tissue injury. Arch Emerg Med 5:223–227

Hull MJ, Abraham JL (2002) Aluminum welding fume-induced pneumoconiosis. Hum Pathol 33:819–825

Kao YY, Chen YC, Cheng TJ, Chiung YM, Liu PS (2012) Zinc oxide nanoparticles interfere with zinc ion homeostasis to cause cytotoxicity. Toxicol Sci 125:462–472

Kermanizadeh A, Gaiser BK, Hutchison GR, Stone V (2012) An in vitro liver model–assessing oxidative stress and genotoxicity following exposure of hepatocytes to a panel of engineered nanomaterials. Part Fibre Toxicol 9:28

Lee J, Kang BS, Hicks B, Chancellor TF Jr, Chu BH, Wang HT, Keselowsky BG, Ren F, Lele TP (2008) The control of cell adhesion and viability by zinc oxide nanorods. Biomaterials 29:3743–3749

Mudunkotuwa IA, Rupasinghe T, Wu CM, Grassian VH (2012) Dissolution of ZnO nanoparticles at circumneutral pH: a study of size effects in the presence and absence of citric acid. Langmuir 28:396–403

Nel A, Xia T, Madler L, Li N (2006) Toxic potential of materials at the nanolevel. Science 311:622–627

Rasmussen JW, Martinez E, Louka P, Wingett DG (2010) Zinc oxide nanoparticles for selective destruction of tumor cells and potential for drug delivery applications. Expert Opin Drug Deliv 7:1063–1077

Sano T (1963) Pathology and pathogenesis of pneumoconiosis. Acta Pathol Jpn 13:77–93

Sayes CM, Reed KL, Warheit DB (2007) Assessing toxicity of fine and nanoparticles: comparing in vitro measurements to in vivo pulmonary toxicity profiles. Toxicol Sci 97:163–180

Tsuda H, Fukamachi K, Ohshima Y, Ueda S, Matsuoka Y, Hamaguchi T, Ohnishi T, Takasuka N, Naito A (2005) High susceptibility of human c-Ha-ras proto-oncogene transgenic rats to carcinogenesis: a cancer-prone animal model. Cancer Sci 96:309–316

Valdiglesias V, Costa C, Kilic G, Costa S, Pasaro E, Laffon B, Teixeira JP (2013) Neuronal cytotoxicity and genotoxicity induced by zinc oxide nanoparticles. Environ Int 55:92–100

Warheit DB, Sayes CM, Reed KL (2009) Nanoscale and fine zinc oxide particles: can in vitro assays accurately forecast lung hazards following inhalation exposures? Environ Sci Technol 43:7939–7945

Xia T, Kovochich M, Liong M, Madler L, Gilbert B, Shi H, Yeh JI, Zink JI, Nel AE (2008) Comparison of the mechanism of toxicity of zinc oxide and cerium oxide nanoparticles based on dissolution and oxidative stress properties. ACS Nano 2:2121–2134

Xu J, Futakuchi M, Iigo M, Fukamachi K, Alexander DB, Shimizu H, Sakai Y, Tamano S, Furukawa F, Uchino T, Tokunaga H, Nishimura T, Hirose A, Kanno J, Tsuda H (2010) Involvement of macrophage inflammatory protein 1 alpha (MIP 1 alpha) in promotion of rat lung and mammary carcinogenic activity of nanoscale titanium dioxide particles administered by intra-pulmonary spraying. Carcinogenesis 31:927–935

Yang H, Liu C, Yang D, Zhang H, Xi Z (2009) Comparative study of cytotoxicity, oxidative stress and genotoxicity induced by four typical nanomaterials: the role of particle size, shape and composition. J Appl Toxicol 29:69–78

The Journal of Toxicological Sciences (J. Toxicol. Sci.)
Vol.38, No.4, 619-628, 2013

Original Article

An improved dispersion method of multi-wall carbon nanotube for inhalation toxicity studies of experimental animals

Yuhji Taquahashi, Yukio Ogawa, Atsuya Takagi, Masaki Tsuji, Koichi Morita and Jun Kanno

Division of Cellular and Molecular Toxicology, Biological Safety Research Center, National Institute of Health Sciences, 1-18-1 Kamiyoga, Setagaya-ku, Tokyo 158-8501, Japan

(Received May 5, 2013; Accepted June 9, 2013)

ABSTRACT — A multi-wall carbon nanotube (MWCNT) product Mitsui MWNT-7 is a mixture of dispersed single fibers and their agglomerates/aggregates. In rodents, installation of such mixture induces inflammatory lesions triggered predominantly by the aggregates/agglomerates at the level of terminal bronchiole of the lungs. In human, however, pulmonary toxicity induced by dispersed single fibers that reached the lung alveoli is most important to assess. Therefore, a method to generate aerosol predominantly consisting of dispersed single fibers without changing their length and width is needed for inhalation studies. Here, we report a method (designated as Taquann method) to effectively remove the aggregate/agglomerates and enrich the well-dispersed singler fibers in dry state without dispersant and without changing the length and width distribution of the single fibers. This method is base on two major concept; liquid-phase fine filtration and critical point drying to avoid re-aggregation by surface tension. MWNT-7 was suspended in Tert-butyl alcohol, freeze-and-thawed, filtered by a vibrating 25 μm mesh Metallic Sieve, snap-frozen by liquid nitrogen, and vacuum-sublimated (an alternative method to carbon dioxide critical point drying). A newly designed direct injection system generated well-dispersed aerosol in an inhalation chamber. The lung of mice exposed to the aerosol contained single fibers with a length distribution similar to the original and the Taquann-treated sample. Taquann method utilizes inexpensive materials and equipments mostly found in common biological laboratories, and prepares dry powder ready to make well-dispersed aerosol. This method and the chamber with direct injection system would facilitate the inhalation toxicity studies more relevant to human exposure.

Key words: Multi-wall carbon nanotube, Dispersion, Metallic sieve, Tert-butyl alcohol, Sublimation, Critical point drying

INTRODUCTION

We previously reported that a certain make of multi-wall carbon nanotube (MWCNT) contained particles similar to asbestos fibers in size and shape, and was positive for mesotheliomagenesis in intraperitoneal injection studies using p53-heterozygous mice (Takagi *et al.*, 2008, 2012). The intraperitoneal injection study is a specialized method for the detection of mesotheliomagenic potential of inhaled fibrous materials (Pott *et al.*, 1994; Roller *et al.*, 1997; Poland *et al.*, 2008). For the assessment of general respiratory toxicity including non-cancerous endpoints, the inhalation studies are considered essential. As a surrogate for inhalation studies, pharyngeal aspiration and intratracheal spray methods are often used. However, in both methods, the suspension medium may modify the distribution and/or the toxicity of the test particles (Morimoto *et al.*, 2011; Oyabu *et al.*, 2011; Gasser *et al.*, 2012; Wang *et al.*, 2012). Dispersion methods without suspension media are reported. However, those are usually using, at least in part of the processes, rigorous sonication or mechanical milling resulting in certain degree of physiological changes in sample characteristics, such as shortening in length distribution of MWNCT (Muller *et al.*, 2005; Mitchell *et al.*, 2007; Ahn *et al.*, 2011). Changes in particle size and/or shape will also affect the nature

Correspondence: Jun Kanno (E-mail: kanno@nihs.go.jp)

and strength of toxicity of the test substances. Therefore, development of a dispersion method to generate the aerosol of concern without addition of chemicals and changes in particle dimensions is considered to be essential for the assessment of inhalation toxicity in humans.

Fibrous nanomaterial such as Mitsui MWNT-7 is a mixture of dispersed single fibers of various length and width, and their agglomerates and aggregates. When given as a mixture, the lung lesions were mainly seen as inflammatory and/or granulomatous lesions with various degree of fibrosis at the level of terminal bronchiole accompanying the aggregates and agglomerates. These lesions were considered to block and/or mask the changes induced by the single fibers that should have reached the alveolar ducts and alveoli (Warheit *et al.,* 2004; Muller *et al.,* 2005; Shvedova *et al.,* 2008; Porter *et al.,* 2009; Mercer *et al.,* 2011; Wang *et al.,* 2011). Therefore, assessment of the toxicity of single fibers needs well-dispersed sample without aggregate/agglomerate. In practical inhalation testing, the animal chamber air is rigorously agitated in order to ensure the homogeneity of aerosol in the chamber. Therefore, if the MWNT-7 as a mixture is used, the likelihood of aggregates/agglomerates reaching the nose of the animals is high. In contrast, human ambient air is less agitated; the aggregates/agglomerates may sediment away fast and dispersed single fibers may stay longer in the air to be inhaled by humans (Han *et al.,* 2008). In addition, humans have longer respiratory tract compared to rodents and may effectively filtered out aggregates/agglomerates before the air reaches the alveolar region.

Taking all into account, we concluded that it is essential to prepare a dispersed single fiber aerosol without aggregate/agglomerates, without additional chemical components, and without changes in size and shape of the single fiber component for the rodent inhalation studies in order to predict human inhalation toxicity. To date, one dispersion method is reported, i.e. the filtration system. Filtration by a sieve with its pore size smaller than the size of aggregates/agglomerate will not affect the size distribution of the single fibers (Kasai *et al.*, 2013). However, filtration in gaseous phase turns out to be ineffective in terms of yield of the filtrate. Filtration in liquid phase is much efficient (Mercer *et al.,* 2008; Tsuda, personal communication). However, in our experience, the difficulty is found in avoiding re-aggregation during the process of drying; the surface tension. To solve this problem, here we report a new improved dispersion method consisting of a combination of aqueous filtering and the concept of a drying method used for scanning electron microscopic (SEM) samples; the critical point drying.

MATERIALS AND METHODS

MWCNT, reagent and equipments

MWCNT (Mitsui MWNT-7) was kindly donated by Mitsui & Co., Ltd., Tokyo, Japan for use in toxicity studies (Takagi *et al.,* 2008). Tert-butanol (TB) of guaranteed reagent grade was used (CAS: 75-65-0, Kanto Chemical Co., Inc., Tokyo, Japan). Metallic Sieve (pore size 25 μm mesh, Seishin Enterprise Co., LTD., Tokyo, Japan) was used for filtration. Miniature coin type vibration motors used in cellular phones (Model FM34F, T.C.P. Co, Tokyo Japan; 13,000 rpm 1.8m²/sec) are attached to the extended filler rim (5cm in depth, custom-made, Seishin Enterprise Co., LTD.) of the metallic sieve (cf. Fig. 1c) to gain high yield of filtrate. Chemistry diaphragm pumps and pumping systems (Model; MD4C NT+AK+EK, Vacuubrand, Wertheim, Germany) was used for sublimation of the frozen TB suspension and recovery of TB. Glass wares such as funnel, filtering bottle, trap bottle and silicon stoppers (Sansyo Co., Ltd., Tokyo, Japan), laboratory bottles (Pyrex®, Asahi Glass Co. Ltd., Tokyo, Japan), were used.

Dispersion method ("Taquann" method)

An outline flowchart is shown in Fig. 1. TB (melting point 25.69°C) was heated up to 60°C by a mantle heater (Sibata Scientific Technology Ltd., Saitama, Japan). It is advised not to use water bath; TB is highly hygroscopic and becomes difficult to freeze and sublimate. A volume of 200 ml of TB and 0.2 g of MWCNT were transferred to a 500 ml laboratory bottle and agitated to make crude suspension. The bottle was put into an ice bath, occasionally shaken by hand, until the suspension starts to freeze and becomes sherbet-like half frozen state and kneaded by a stainless steel spatula until it becomes evenly gray without clear crystals of TB (Fig. 1a), and then kept overnight at -25°C. To the frozen suspension, 500 ml of TB pre-heated to 60°C, was added, capped and shaken hard until the liquefied suspension becomes evenly dark brown to gray in color (Fig. 1b). The bottle was further heated up to 60°C by a mantle heater and the suspension was immediately applied to vibrating metal sieve for filtration (Fig. 1c). The filtrate was collected through a funnel into a 1,000 ml laboratory bottle. Immediately after the filtration, approximately 1,500 ml of liquid nitrogen was poured onto the filtrate in the bottle to snap freeze the suspension (Fig. 1d). Then, the bottle was connected to the pumping system and vacuumed until TB was totally sublimated; leaving dispersed MWCNT (T-CNT for Taquann-treated MWCNT) in the bottle. The MWCNT was collected by a cyclone-suction bottle using conduc-

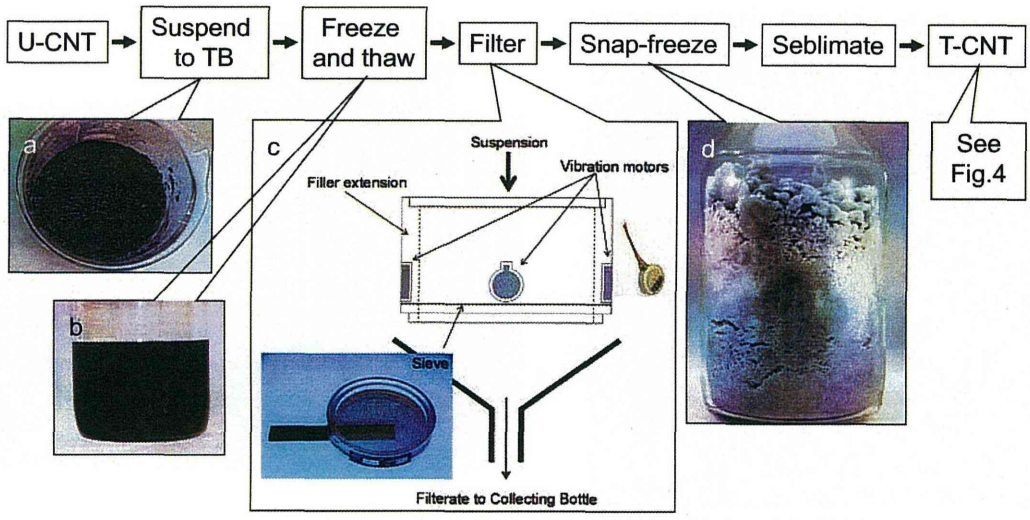

Fig. 1. Outline flowchart of the Taquann method. a) Half-frozen sherbet-like suspension of MWNT-7 kneaded (beaker was used for demonstration). b) Well-shaken liquefied suspension after adding 60°C TB (beaker was used for demonstration). c), Photograph of the sieve on a backlight box with a scale underneath (left inset), vibration motor (right inset), and a diagram of the filter unit with a filler extension and vibration motors. d) Snap-frozen filtrate.

tive silicon and aluminum tubing. In order to make a precise aliquot, a measured amount the collected T-CNT was resuspended to TB, and the suspension was aliquoted into proper containers, in this study into the newly designed cylindrical cartridge case (cf. Fig. 3), snap-frozen, and sublimated.

Aerosol generation system

An originally designed 105 L main exposure chamber (capacity of 16 mice per chamber), with a disposable electrostatic-free plastic bag inside, was prepared (Fig. 2, patent pending, manufactured by Sibata Scientific Technology Ltd.). Onto the plastic disposable top plate, a 20 L subchamber was connected with a 5 cm-diameter 10 cm long connecting pipe. To the subchamber, an injection port was connected, to which a newly designed cylindrical cartridge (manufactured by Sibata Scientific Technology Ltd.) containing dispersed T-CNT is loaded. The cartridge has a slide-valve air inlet at its base and four ejection holes at its top opening towards the subchamber lumen. The compressed air (0.8 M pascal) was injected five times with 0.2 sec duration and 10 sec interval to empty the T-CNT into the subchamber (Fig. 3). The carrier air flow from the subcamber to the main chamber was 15 L/min. Twenty-one cartridges were prepared for a two-hr exposure experiment, loading first two in 1 min for an initial boost and then one in every 6 min, resulting in generation of saw-tooth concentration wave with an average of 1.3 mg/m^3 (250 μg/cartridge) and 2.8 mg/m^3 (500 μg/cartridge).

Twelve C57BL/6NCrSlc male mice (SLC, Inc., Shizuoka, Japan), 10~11 weeks old, body weight of 23.8~30.8 g were placed in the cage suspended from the top plate of the inhalation chamber and exposed to 1 mg/m^3 of T-CNT for 2 hr a day for 5 days, lungs (excluding primary bronchi) were sampled and subjected to characterization of deposited fibers (see below).

The animal study was conducted in accordance with the Guidance for Animal Studies of the National Institute of Health Sciences under Institutional approval.

Real time particle counting and weight measurement

An optical particle counter (OPC) with a nominal detection limit of 300 nm (OPC-110GT, Sibata Scientific Technology Ltd.) and a condensation particle counter (CPC) with a nominal detection limit of 2.5 nm (ultrafine condensation particle counter 3776, Trust Science Innovation, MN, USA) were connected to the main chamber with a sample flow of 2.83 L (0.1cf) /min and 0.3 L/min respectively. The mass concentration of the chamber aerosol was calculated from the weight increase of polytetrafluoroethylene-glass fiber filter (Model T60A20, φ55mm, Tokyo Dylec Corp, Tokyo, Japan) after filtering the chamber aerosol by an Asbestos sampling pump (AIP-105, Sibata Scientific Technology Ltd.) at a rate of 1.5 L/min for 120 min (total of 180 L). Filter weight was measured by a microbalance (XP26V,

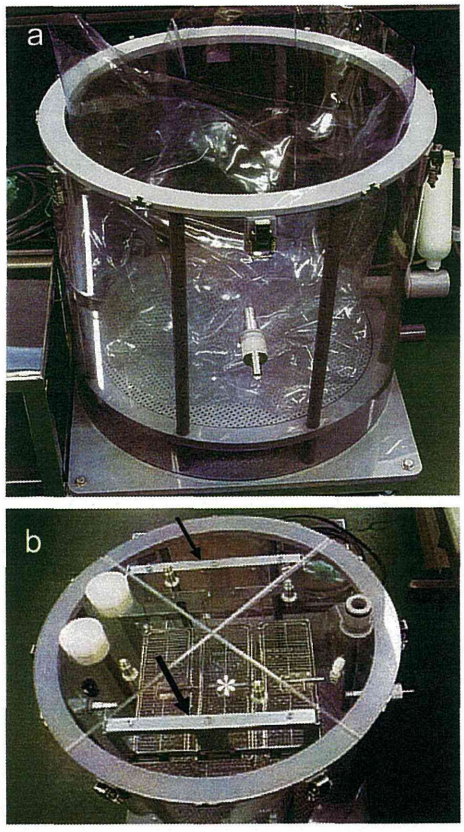

Fig. 2. Newly designed original inhalation chamber. a) Outer chamber and inner bag before top plate is in place. During operation, the space between the outer chamber and inner bag is negatively pressured to inflate the inner bag. B) Disposable top plate with tubing holes are placed on the chamber. The animal cages for 16 mice (asterisk) are suspended from the top place by a pair of hanger arms (arrows) (photo was taken without inner bag for better demonstration).

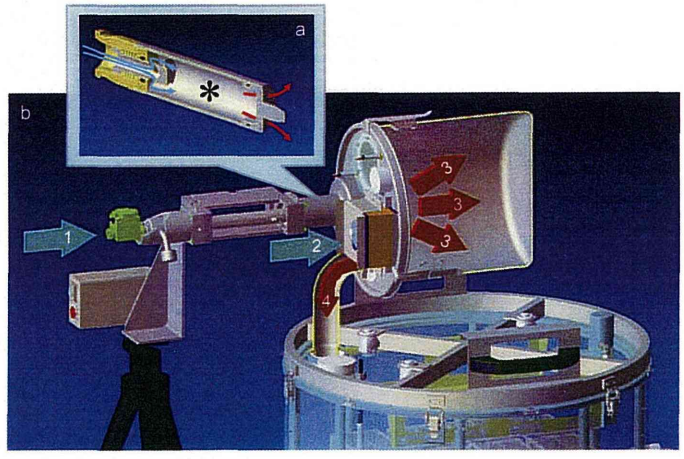

Fig. 3. A scheme of direct injection aerosol generation system. a) Upper inset shows the cut section of the injection cartridge (capacity; 23.5 ml). A slide valve opens when the cartridge is loaded to the subchamber. A measured amount of dispersed MWCNT is preloaded inside the cartridge shown in asterisk. b) Compressed air (Blue arrow 1) blows out the MWCNT through four small outlets of the cartridge into the subchamber (red arrows 3), where main flow air from the HEPA filtered inlet (blue arrow 2) mixes in. The air with the aerosol goes down the connection pipe to the main chamber (red arrow 4).

Mettler Toledo).

Characterization of the dispersed MWCNT

The T-CNT in TB suspension was mounted on a slide glass and observed under a light microscope using a pair of polarizing filters. Untreated MWCNT (U-CNT) from the bulk, 200 mg, was dispersed in to 500 ml of TB and sonicated for 30 min at 40W, 3.4 kHz (SU-3TH, Sibata Scientific Technology Ltd.) and observed.

A weight-measured aliquot of T-CNT was re-suspended, blotted on a Anopore™ Inorganic Aluminum Oxide Membrane Filters (Whatman GmbH, Dassel GE Healthcare, Hahnestrasse, Germany, pore size; 0.02 μm, φ13 mm, Anodisc 13) or a cellulose acetate/nitrocellulose membrane filter (MFTM- Millipore Membrane filters, 0.025 μm, φ13 mm, Merck Millipore, Billerica, MA, USA) and observed with a scanning electron microscope (SEM).

From the main chamber, the aerosol was collected at a rate of 5 L/min for 3 min on a Anopore™ Inorganic Aluminum Oxide Membrane Filters (Whatman GmbH, pore size; 0.1 um, Anodisc 25) joined to asbestos sampling pump (AIP-105, Sibata, Scientific Technology Ltd.). A scanning electron microscope (SEM) (VE-9800, Keyense Co., LTD., Osaka, Japan) was used for monitoring the details of the samples on the slide glasses and on the Anodiscs after osmium coating (HPC-1SW, Vacuum Device Inc., Ibaraki, Japan).

From the exposed mouse, lung lobes are collected and treated with lysis solution composed of 5 w/v% potassium hydroxide (Super Special Grade, Wako Pure Chemical Industries, Ltd., Osaka, Japan), 0.1w/v% Sodium dodecyl sulfate (SDS, for Biochemistry, Wako Pure Chemical Industries, Ltd.), 0.1 w/v% Ethylenediamine-N,N,N',N'-tetraacetic acid disodium salt dehydrate (EDTA 2Na, Dojindo laboratories, Kumamoto, Japan) and 2w/v% ascorbic acid (Super Special Grade, Wako Pure Chemical Industries, Ltd.) in ultra-pure water, dissolved at 80°C (Fig. 10b). Lung samples (approx. 200 mg) and 1.8 ml of

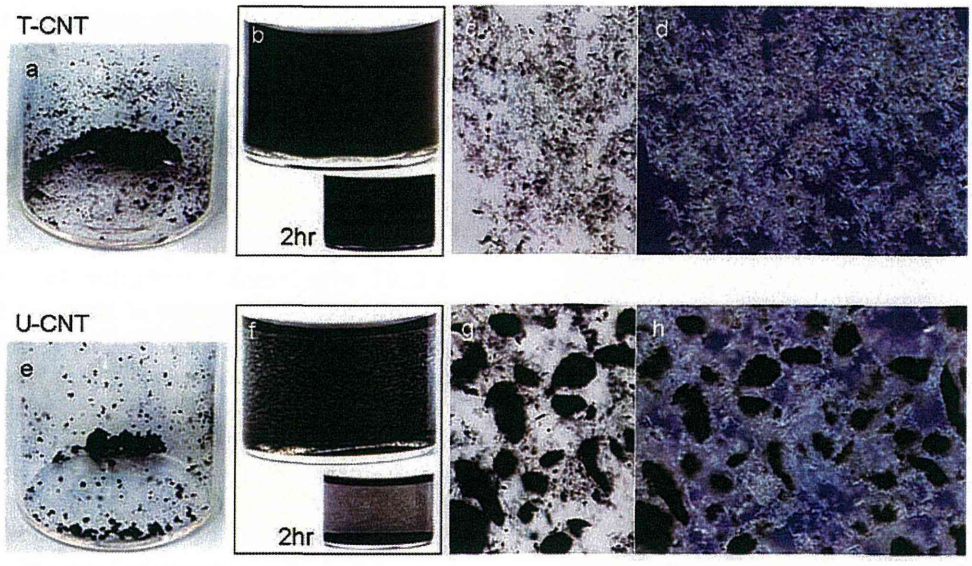

Fig. 4. Taquann-treated carbon nanotube (T-CNT) and untreated bulk carbon nanotube (U-CNT). a) final fine and dry powder of Taquann-treated MWCNT. b) Resuspended T-CNT to TB and placed for 5 min and 2 hr; T-CNT suspension is stable, compared to U-CNT, c) light microscopic view of the resuspended T-CNT on a slide glass, and d) under polarized light. e) course powder of U-CNT, f) Resuspended U-CNT to TB and placed for 5 min and 2 hr. g) light microscopic view of the resuspended U-CNT on a slide glass, and d) under polarized light. (diameter of the vials in a), b), e) and f) is 2.3 cm)

lysis solution in a centrifuge tube (DNA LoBindid tube 2.0 ml, Eppendorf, Hamburg, Germany) was incubated at 80°C for approx. 24 hr in an oven (HV-100, Funakoshi Co., Ltd., Tokyo, Japan), centrifuged at 20,000 g for 1 hr at 25°C (MX-207, Tomy Seiko Co., Ltd., Tokyo, Japan), and the pellet containing MWCNTs and SDS crystals was recovered. 1.8 ml of 70% ethanol was added to the tube and incubated at 80°C for 30 min to dissolve SDS crystals and centrifuged at 20,000 g for 1 hr at 25°C. 100 µl of 1w/w% Triton®X-100 (MP Biomedicals, Inc., Solon, OH, USA) was added to the pellet and dispersed by pipetting. One microliter of the suspension was placed on an inorganic aluminum oxide membrane filter (Anodisc 13, 0.02 µm φ13mm, Whatman GmbH) or the cellulose acetate/nitrocellulose membrane filter and filtrated on a funnel shape glass filter (SANSYO Co., LTD., Tokyo, Japan). The filter was dried at room temperature and osmium coated for SEM. For a reference of extraction efficiency, lung sample from untreated mouse was spiked with 1 µg T-CNT and measured alongside.

Lung tissue from eight mice were fixed with buffered 10% formalin (four with and four without inflation), paraffin embedded and processed routinely for H&E stained histology slides, and observed under a light microscope with or without polarizing filters (Olympus BX50 microscope with DP-70 image system, Olympus Corporation, Tokyo, Japan).

RESULTS

Characteristics of "Taquann"-dispersed MWCNT

Macroscopic and light microscopic views of the final product, the dried MWCNT after sublimation, i.e. "Taquann"-dispersed MWCNT (T-CNT) and, for comparison, untreated MWCNT from the bulk (U-CNT) are shown in Fig. 4. The powder of T-CNT is finer compared to U-CNT (Fig. 4a). The T-CNT resuspended very well to TB (Fig. 4b) and other solvents including 0.1 w/v% Sodium dodecyl sulfite and 0.1 w/v% Sodium dodecylbenzene sulfonate (not shown). Light microscopically, the resuspended T-CNT consists mostly of dispersed single fibers with smaller numbers of small aggregates corresponding to the mesh size of the metal sieve (Figs. 4c, 4d), whereas U-CNT was a mixture of large aggregates/agglomerates and single fibers among them (Figs. 4g, 4h). The T-CNT fibers slowly precipitated in the medium (cf. Figs. 4b and f), and are easily resuspended by gentle agitation. The yield of the T-CNT was approximately 5% of the U-CNT in weight. Re-filtration of the residue on the sieve resulted in negligible yield. The low power SEM views of the TB-resuspended T-CNT and U-CNT are shown in Fig. 5.

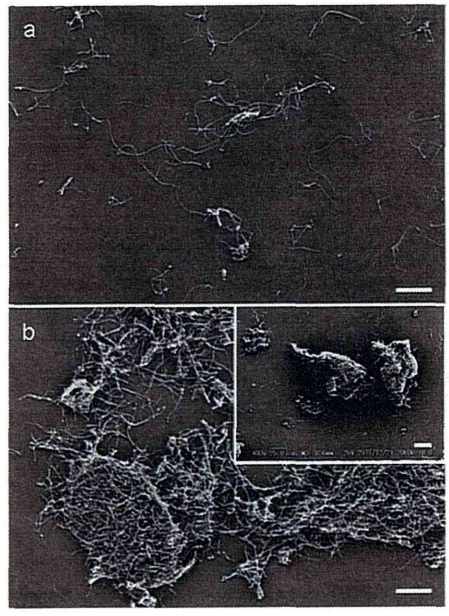

Fig. 5. Scanning electron microscopy of T-CNT and U-CNT re-suspended in TB. a) T-CNT consists mainly of dispersed single fibers with few small aggregates/agglomerates smaller than the mesh size of the sieve, SEM x 1,000. b) U-CNT showing mixture of single fibers and large aggregates/agglomerates, SEM x 1,000. The length and width distribution of the single fibers of T-CNT were virtually identical to those of U-CNT. Inset; Lower power view to demonstrate larger aggregates/agglomerates measuring up to 300 μm in major axis SEM x 400. (scale bars are 10 μm)

Again, the majority of the particles of the T-CNT were the dispersed single fibers. The length and width distribution of single fibers counted on these SEM images are shown in Fig. 6. The length and width distribution was similar between single fibers of T-CNT and U-CNT, indicating that the mechanical shortening of the fibers is negligible for Taquann method.

The number of fibers per 10, 1 and 0.1 μg weight of T-CNT with length distribution was counted on SEM images (measured number of fibers are 959, 246, and 45 per designated area for calculation, respectively). The number of fibers calculated was 2.1 x 10^7/10 μg 4.1 x 10^6/1 μg and 3.3 x 10^5/0.1 μg. The distribution of the fiber length was similar to that shown in Fig. 6a, and the average length was 7.5 ± 4.7 μm (max 34 μm), 8.7 ± 6.4 μm (max 42 μm), and 7.0 ± 5.4 μm (max 26 μm) respectively. As a whole, T-CNT has roughly 3 x 10^6 fibers per 1 μg, mean length of approximately 7 μm with a length range up to 50 μm with a median of approximately 6.5 μm.

"Taquann"-dispersed MWCNT in the inhalation chamber

The T-CNT aerosol generated at an average concentration of 1 mg/m³ was sampled on the Anodisc and observed by a SEM (Fig. 7). The aerosol was composed mainly of well-dispersed single fibers and some small tangles of fibers admixed with a relatively small amount of non-fibrous particles.

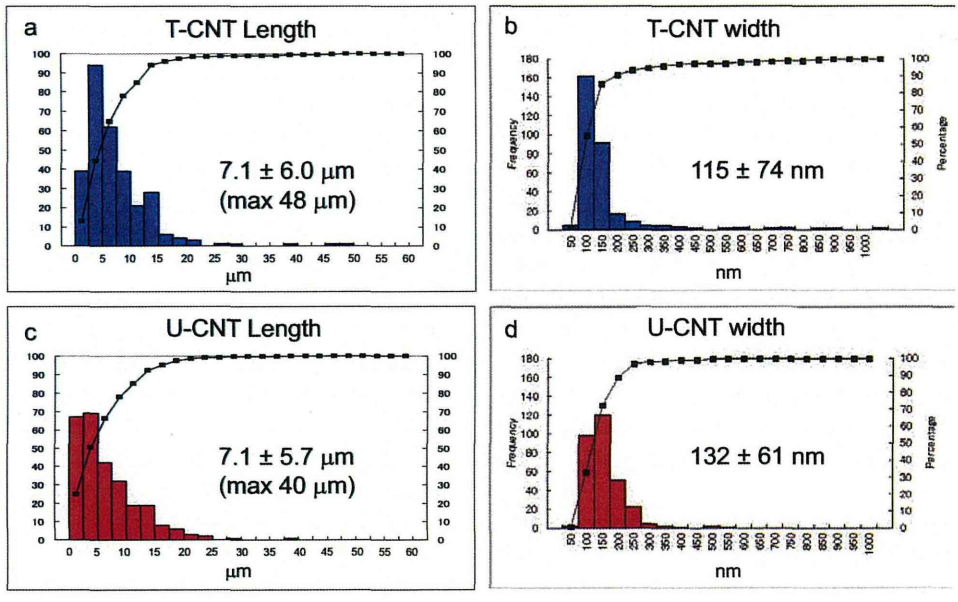

Fig. 6. Length and width of single fibers in T-CNT and U-CNT (measured by SEM on TB-resuspended samples). a) Length distribution and b) width distribution of Taquann-treated MWNT-7. c) Length distribution and d) width distribution of single fibers in the mildly sonicated suspension of the bulk MWNT-7 (mean ± s.d., n = 304 each).

Table 1. Aerosol particle count by optical particle counter (OPC) and condensation particle counter (CPC).

	Date of measurement	2013/4/29	2013/5/1	2013/5/3
Equipment	Mass concentration (mg/m³)	1.25	1.25	1.38
OPC	Average cpm* (/L) ± s.d.	627,096 ± 145,399	781,973 ± 138,610	821,272 ± 114,278
	K-value (mg/m³/cpm)	1.99×10^{-9}	1.60×10^{-9}	1.68×10^{-9}
CPC	Average cpm (/L) ± s.d.	859,692 ± 171,858	1,228,545 ± 223,371	1,317,873 ± 217,990
	K-value(mg/m³/cpm)	1.45×10^{-9}	1.02×10^{-9}	1.05×10^{-9}

*count per minute

Fig. 7. T-CNT aerosol at a concentration of 1 mg/m³ in the main chamber was collected on the Anodisc filter (5 L/min for 3 min). SEM x 1,000. (scale bar is 10 μm)

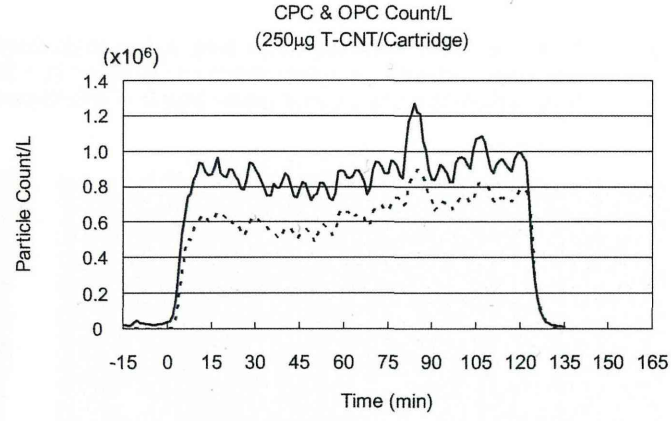

Fig. 8. A real time data from condensation particle counter (CPC, solid line) and optical particle counter (OPC, dotted line) from an inhalation chamber injected with T-CNT (250 μg/cartridge) from 0 min to 120 min with an average injection interval of 6 min (for detail see text).

From the amount of weight increase of polytetrafluoroethylene-glass fiber filter after sampling the chamber aerosol, the weight of aerosol per m³ of the chamber air (weight concentration) was calculated as approximately 1.3 mg/m³ (average of three measurements shown in Table 1). At the same time, the particle counts per m³ given by OPC and CPC were recorded (Fig. 8), and the K-value (mg/particle count in m³) was calculated (Table 1).

K-value (mg/m³/cpm), i.e. the weight concentration (mg/m³) divided by OPC or CPC count per minute (cpm) is often used as an indicator of the status of dispersion. Three measurements conducted with a few days' interval showed that not only the K-values itself but also the values used to calculate it were fairly stable over a period of days.

The length distribution of the T-CNT recovered from the lungs of two mice exposed in the whole body inhalation chamber 2 hr a day for 5 days at an average concentration of 1.8 mg/m³ of T-CNT are shown in Fig. 9 along with the data from the spiked lung tissue sample. The average length were 8.4 ± 5.0 μm and 8.3 ± 4.9 μm (Figs. 9a, 9b), comparable to that of the T-CNT in spiked lung tissue sample; 9.5 ± 5.2 μm (Fig. 9c) (width was qualitatively not different, data not shown). The total numbers of the fibers recovered were 5.1×10^6 and 3.2×10^6 from the inhaled lungs and 1.6×10^6 from the spiked lung; the weight of T-CNT deposited in the lung after 2 hr x 5 days of inhalation was roughly calculated as 3 μg/lung.

The fibers recovered from one of the mice were observed with SEM (Fig. 10a). Dispersed single fibers were found and some of which are longer that 20 μm (cf. Fig. 9). It was noted that EDTA and ascorbic acid in the lysis solution were effective in removing the debris from the SEM sample (Fig. 10b).

Histologically, the CNTs were found to distribute from bronchial lumen to peripheral alveolar spaces. In the bronchial lumen, the fibers were trapped in the bronchial mucus, either as single fibers or as loose aggregates